

**The importance of aromaticity to describe the interactions of organic matter
with carbonaceous materials depends on molecular weight and sorbent
geometry**

Supporting information

*Stephanie Castan¹, Gabriel Sigmund¹, Thorsten Hüffer¹, Nathalie Tepe¹, Frank von der Kammer¹,
Benny Chefetz², Thilo Hofmann^{1*}*

*1 Environmental Geosciences, Centre for Microbiology and Environmental Systems Science,
University of Vienna, Althanstraße, 1090 Wien, Austria. E-mail: thilo.hofmann@univie.ac.at*

*2 Department of Soil and Water Sciences, Faculty of Agriculture, Food and Environment, The
Hebrew University of Jerusalem, P.O. Box 12, Rehovot 7610001, Israel*

Number of pages: 12

Number of tables: 2

Number of figures: 6

Abbreviations

CDOM	Compost Dissolved Organic Matter
DOC	Dissolved Organic Carbon
DOM	Dissolved Organic Matter
FI	Fluorescence Index
FT-IR	Fourier Transform Infrared
HA	Humic Acid
SEC	Size Exclusion Chromatography
SRNOM	Suwannee River Natural Organic Matter
SSA	Specific Surface Area

Supplementary Figures

- Figure S1 FT-IR spectra for biochar, graphite, and carbon nanotubes
- Figure S2 Five molecular weight fractions of DOM according to preferential adsorption
- Figure S3 SEC chromatograms of CDOM, SRNOM and HA before and after sorption, detected by fluorescence (ex. 350 nm, em. 450 nm)
- Figure S4 SUVA₂₅₄ value, E₂/E₃ ratio, FI value, and Peak C:B ratio of CDOM, SRNOM and HA divided into five molecular weight fractions
- Figure S5 SEC chromatograms of CDOM, SRNOM and HA, detected by fluorescence (ex. 270 nm, em. 350 nm) and by UV (254 nm)
- Figure S6 N₂ pore size distribution of biochar, graphite and carbon nanotubes

Supplementary Tables

Table S1 Sorbent and sorbate characterization

Table S2 DOC, UV absorption and SUVA₂₅₄ of five DOM fractions

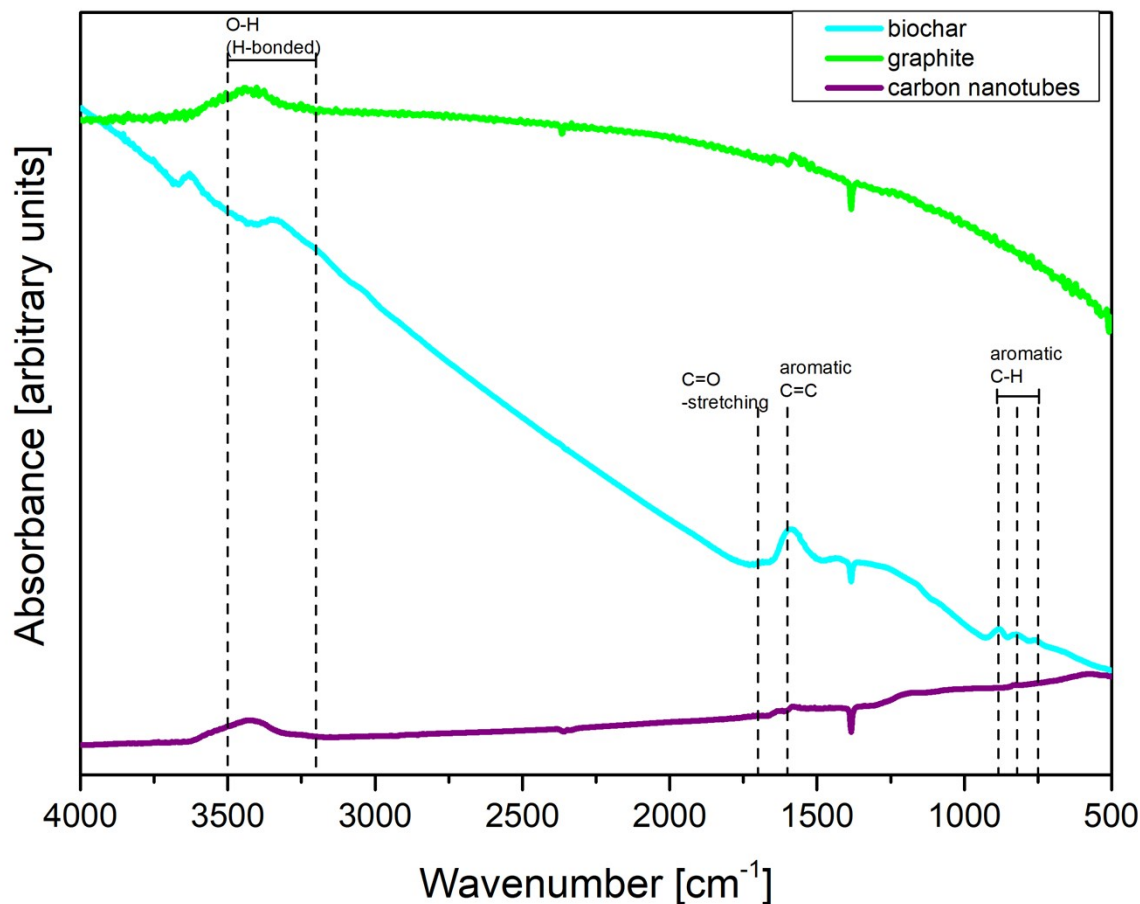


Figure S1. Fourier transform infrared (FT-IR) spectra for biochar (— blue line), graphite (— green line), and carbon nanotubes (— purple line). Spectra were recorded on a Bruker Tensor 27. CMs were embedded in KBr pellets, peak assignments according to Keiluweit et al. (2010).¹

Carbon nanotubes and graphite showed a featureless spectrum as already reported in previous studies (e.g., Chang et al. (2012)²). The common peak for all sorbents (3200-3500 cm⁻¹) is due to hydrogen-bonded O-H stretching of water molecules. Biochar was confirmed to have a high degree of carbonization as the three bands between 885 and 750 cm⁻¹ provide evidence for aromatic C (out-of-plane deformations of aromatic C-H) as well as a pronounced peak at 1600 cm⁻¹ (aromatic C=C).¹ Indications for functional groups may include the peak at 3645 cm⁻¹ (O-H stretching, indicating alcoholic or phenolic groups) and the C=O stretching at 1700 cm⁻¹ indicating the

presence of hydroxyl groups. A previous study measuring FT-IR of the same biochar material (SWP700) furthermore reported C=O functional groups ($\sim 1640\text{ cm}^{-1}$) and aliphatic CH₃ ($\sim 1380\text{ cm}^{-1}$) and C-O-C (1130 cm^{-1}).³ Further peaks measured for the same biochar were assigned to C-C and C-O stretching (1118 cm^{-1} and 1182 cm^{-1} , respectively) as well as CH₂ groups (1437 cm^{-1} and 1490 cm^{-1}).⁴

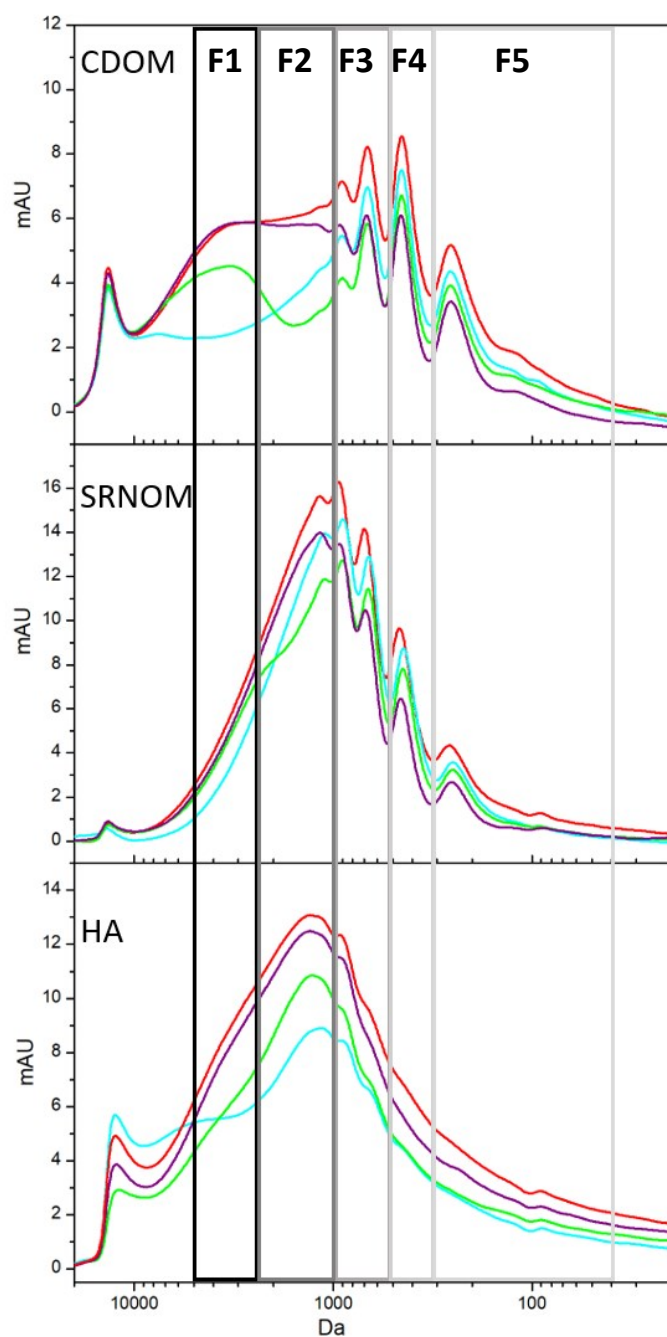


Figure S2: Division of DOM molecular weight into 5 fractions according to preferential adsorption by biochar (— blue line), graphite (— green line), and carbon nanotubes (— purple line). Each sorbent preferentially sorbed distinct molecular weight fractions of the DOM, which were then categorized as fractions 1 – 5 (F1-F5). Each fraction was collected and further characterized.

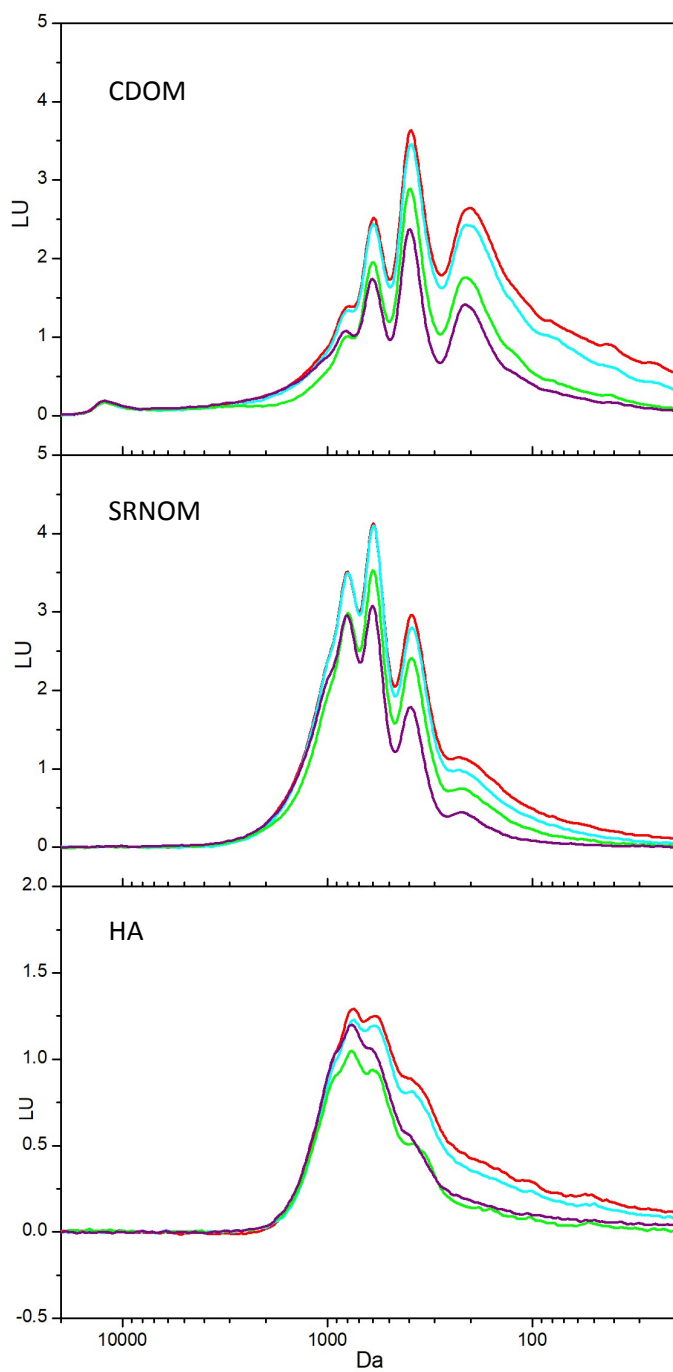


Figure S3. SEC chromatograms of CDOM, SRNOM and HA, detected by fluorescence (excitation wavelength 350 nm, emission wavelength 450 nm) prior to sorption (— red line), and after sorption to biochar (— blue line), graphite (— green line), and carbon nanotubes (— purple line).

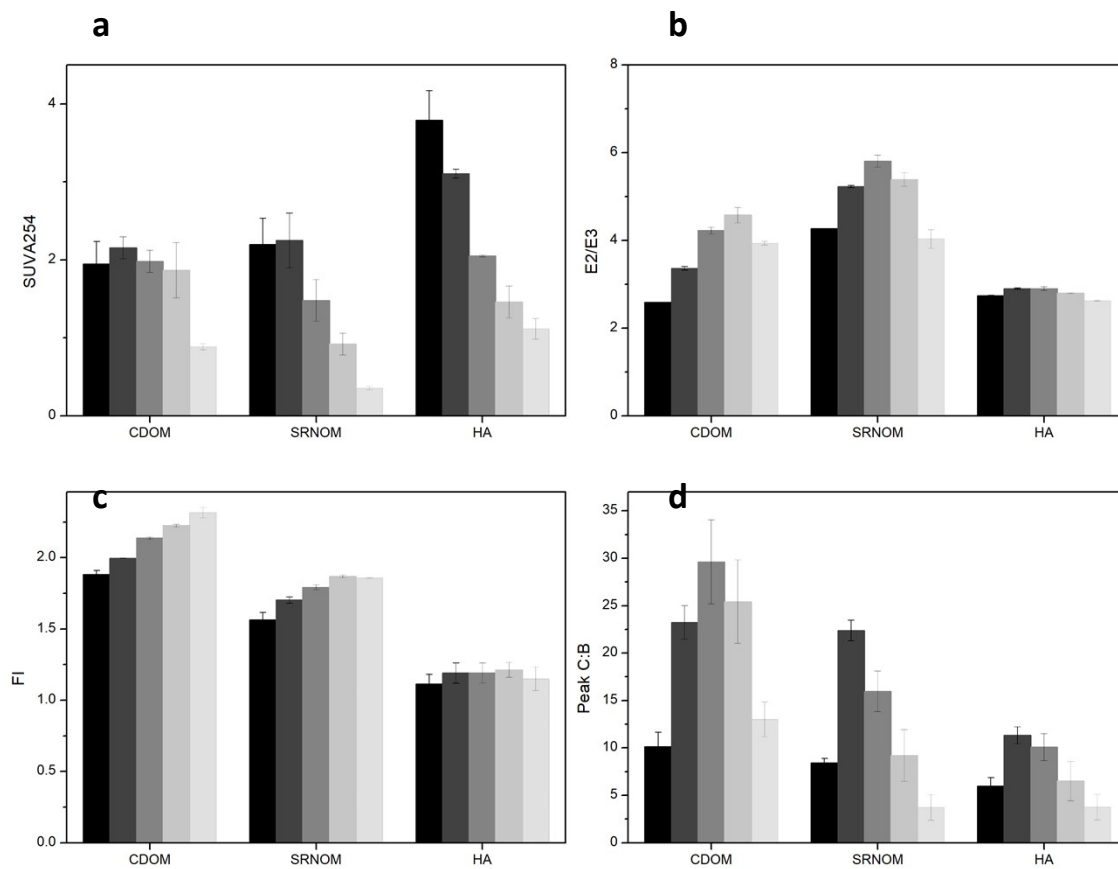


Figure S4. a) SUVA₂₅₄ value, b) E₂/E₃ ratio, c) FI value, and d) Peak C:B ratio of CDOM, SRNOM and HA divided into five molecular weight fractions: 5 – 2.5 kDa (—), 2.5 – 1 kDa (—), 1 – 0.5 kDa (—), 0.5 – 0.3 kDa (—), and 0.3 – 0.03 kDa (—). The error bars represent the standard deviation from duplicate measurements.

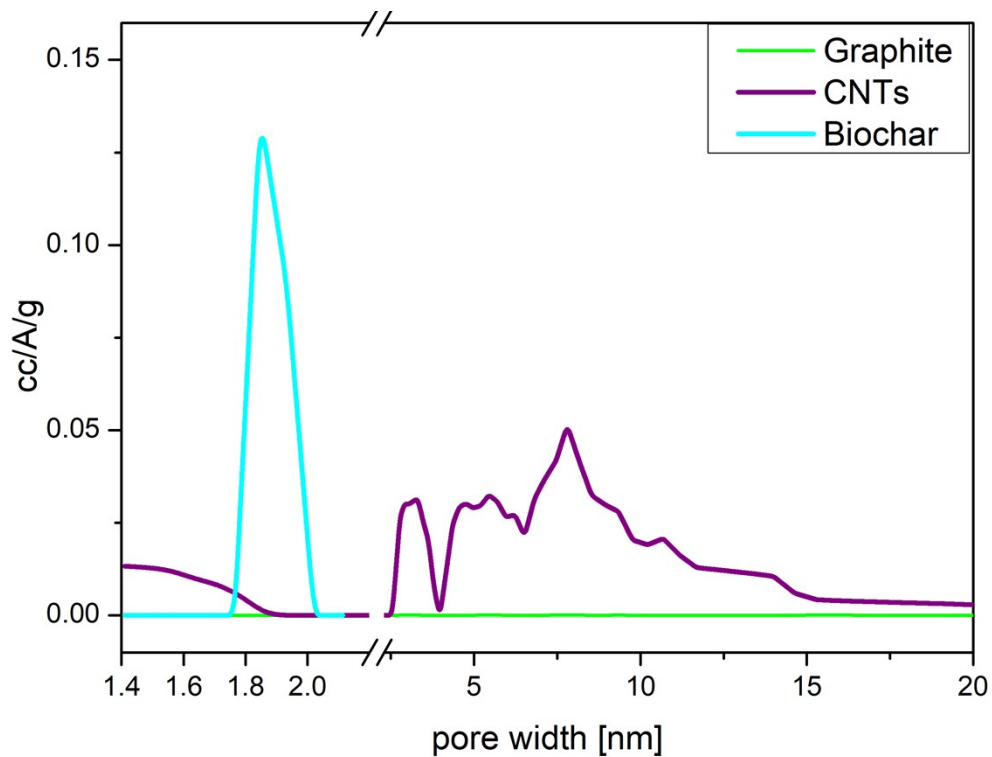


Figure S5. N₂ pore size distribution of biochar (— blue line), graphite (— green line), and carbon nanotubes (— purple line).

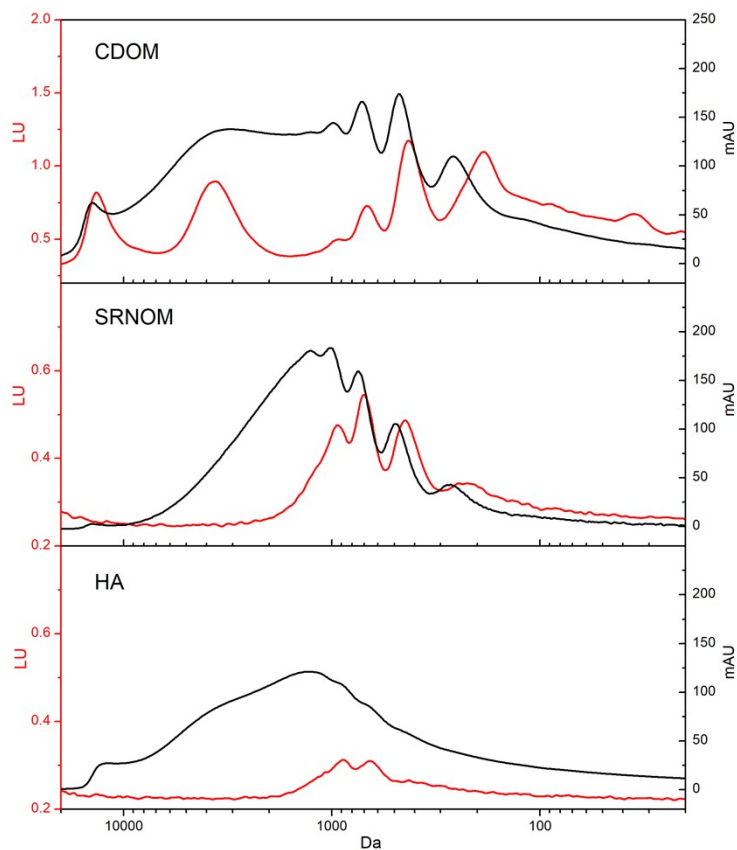


Figure S6. SEC chromatograms of CDOM, SRNOM and HA, detected by fluorescence at an excitation wavelength of 270 nm and an emission wavelength of 350 nm (— red line), and by UV at a wavelength of 254 nm (— black line). The peak in the molecular weight fractions > 2.5 kDa and < 4 kDa in CDOM indicates the presence of protein-like and tryptophan-like compounds in this molecular weight fraction, which also applies for the smaller fraction < 1 kDa.

Table S1. Sorbent and sorbate characterization.

	C [%]	H [%]	O [%]	N [%]	S [%]	Ash content [%]	Size	SSA N ₂ [m ² /g]
SRNOM ^a	50.7	4.0	41.5	1.3	1.8	4.01	n.d.	n.d.
HA	38.9	3.3	24.4	1.0	0.6	31.9	n.d.	n.d.
CDOM	24.6	3.0	n.d.	7.9	2.5	n.d.	n.d.	n.d.
Biochar	91.5	1.4	4.6	0.4	0.1	1.89 ^b	64-250 μm	132.1
Graphite	100.0	n.d.	n.d.	n.d.	n.d.	n.d.	< 150 μm	3.4
SWCNTs	≥ 95	n.d.	n.d.	n.d.	n.d.	n.d.	0.78 nm	704.8

^a IHSS, Elemental analyses by Huffman Laboratories, Wheat Ridge, CO, USA,

^b UK Biochar Research Centre

n.d. = not determined

	C [%]	H [%]	O [%]	N [%]	S [%]	Ash content [%]	Size	SSA N ₂ [m ² /g]	SUVA ₂₅₄
SRNOM ^a	50.7	4.0	41.5	1.3	1.8	4.01	n.d.	n.d.	4.0
HA	38.9	3.3	24.4	1.0	0.6	31.9	n.d.	n.d.	8.7
CDOM	24.6	3.0	n.d.	7.9	2.5	n.d.	n.d.	n.d.	3.0
Biochar	91.5	1.4	4.6	0.4	0.1	1.89 ^b	64-250 μm	132.1	n.d.
Graphite	100.0	n.d.	n.d.	n.d.	n.d.	n.d.	< 150 μm	3.4	n.d.
SWCNTs	≥ 95	n.d.	n.d.	n.d.	n.d.	n.d.	0.78 nm	704.8	n.d.

^a IHSS, Elemental analyses by Huffman Laboratories, Wheat Ridge, CO, USA,

^b UK Biochar Research Centre

n.d. = not determined

Table S2. DOC [mg/L], UV absorption at 254 nm, and SUVA₂₅₄ of five DOM fractions, divided according to preferential adsorption (Fig S2).

	DOC [mg/L]	abs at 254 nm	SUVA ₂₅₄
CDOM			
Fraction 1	6.83 ± 1.02	0.131 ± 0.001	1.9 ± 0.3
Fraction 2	6.68 ± 0.54	0.143 ± 0.002	2.1 ± 0.1
Fraction 3	6.06 ± 0.53	0.119 ± 0.002	2.0 ± 0.1
Fraction 4	5.08 ± 1.11	0.091 ± 0.003	1.8 ± 0.4
Fraction 5	4.50 ± 0.35	0.040 ± 0.001	0.9 ± 0.0
SRNOM			
Fraction 1	5.39 ± 0.81	0.116 ± 0.000	2.1 ± 0.3
Fraction 2	6.45 ± 1.02	0.141 ± 0.000	2.2 ± 0.4
Fraction 3	5.83 ± 1.10	0.083 ± 0.001	1.4 ± 0.3
Fraction 4	5.04 ± 0.93	0.045 ± 0.002	0.9 ± 0.1
Fraction 5	4.22 ± 0.55	0.015 ± 0.001	0.4 ± 0.0
HA			
Fraction 1	4.63 ± 0.39	0.174 ± 0.003	3.8 ± 0.4
Fraction 2	4.94 ± 0.10	0.153 ± 0.000	3.1 ± 0.1
Fraction 3	4.60 ± 0.02	0.094 ± 0.000	2.1 ± 0.0
Fraction 4	4.86 ± 0.64	0.070 ± 0.001	1.4 ± 0.2
Fraction 5	3.84 ± 0.30	0.042 ± 0.002	1.1 ± 0.1

References:

1. Keiluweit, M., Nico, P. S. & Johnson, M. G., Dynamic Molecular Structure of Plant Biomass-Derived Black Carbon (Biochar), *Environ. Sci. Technol.*, 2010, **44**, 1247–1253
2. Chang, C.-H. *et al.*, Novel anticorrosion coatings prepared from polyaniline/ graphene composites, *Carbon N. Y.*, 2012, **50**, 5044–5051
3. Alozie, N., Heaney, N. & Lin, C., Biochar immobilizes soil-borne arsenic but not cationic metals in the presence of low-molecular-weight organic acids, *Sci. Total Environ.*, 2018, **630**, 1188–1194
4. Heaney, N., Mamman, M., Tahir, H., Al-Gharib, A. & Lin, C., Effects of softwood biochar on the status of nitrogen species and elements of potential toxicity in soils, *Ecotoxicol. Environ. Saf.*, 2018, **166**, 383–389